

after several algebraic manipulations, we obtain

$$I_s(u_1, u_2) = ie^{-iku_1}\psi_v^*(u_1) - ie^{-iku_2}\psi_v^*(u_2), \quad u_1 > 0 \quad (7)$$

$$I_v(u_1, u_2) = [2(\pi)^{1/2}/\Gamma(\nu)](k/2)^\mu k_\mu(k) + ie^{ik|u_1|}\psi_v(|u_1|) - ie^{-iku_2}\psi_v(u_2), \quad u_1 < 0 \quad (8)$$

Equations (7) and (8) give a simple and direct way for the evaluation of the nonelementary part of the supersonic Kernel, in terms of the real function $F_v(u)$.

Conclusions

Simple and direct expressions for the evaluation of the nonelementary part of the Kernel function of the integral equation relating the pressure and the normal wash distribution in supersonic nonstationary flow has been presented. It has been shown that the solutions presented are related to the same functional solutions of the subsonic Kernel. The expressions presented here can provide the basis for the development of numerical nonstationary interfering lifting surface methods.

References

- ¹Kussner, H. G., "Allgemeine Tragflächentheorie," *Luftfahrtforschung*, Vol. 17, No. 11-12, 1940, pp. 370-379; also, "General Airfoil Theory," NACA TM-979, 1941.
- ²Watkins, C. E., and Berman, J. H., "On the Kernel Function of the Integral Equation Relating Lift and Downwash Distributions of Oscillating Wings in Supersonic Flow," NACA Rept. 1257, 1956.
- ³Watkins, C. E., Ruyan, H. L., and Woolston, D. S., "On the Kernel Function of the Integral Equation Relating the Lift and Downwash Distribution of Oscillating Finite Wings in Subsonic Flows," NACA Rept. 1234, 1955.
- ⁴Laschka, B., "Zur Theorie der Harmonischen Schwingenden Tragenden Fläche bei Unterchallanströmung," *Zeitschrift für Flugwissenschaften*, Vol. 11, No. 7, 1963, p. 265-292.
- ⁵Landahl, M. T., "Kernel Function for Nonplanar Oscillating Surfaces in Subsonic Flow," *AIAA Journal*, Vol. 5, No. 5, 1967, pp. 1045-1046.
- ⁶Albano, E., and Rodden, W. P., "A Doublet-Lattice Method for Calculating Lift Distributions on Oscillating Surfaces in Subsonic Flows," *AIAA Journal*, Vol. 7, No. 2, 1969, pp. 279-285.
- ⁷Harder, R. L., and Rodden, W. P., "Kernel Function for Nonplanar Oscillating Surfaces in Supersonic Flow," *Journal of Aircraft*, Vol. 8, No. 8, 1971, pp. 667-669.
- ⁸Bismarck-Nasr, M. N., "On the Kernel Function Occurring in Subsonic Unsteady Potential Flow," *AIAA Journal*, Vol. 29, No. 6, 1991, pp. 878, 879.
- ⁹Bismarck-Nasr, M. N., "On Some Integral Representations of the Kernel Function Occurring in Unsteady Subsonic Potential Flows," *Journal of the Brazilian Society of Mechanical Sciences* (submitted for publication).

Extensions to the Minimum-State Aeroelastic Modeling Method

Mordechay Karpel*

Technion—Israel Institute of Technology,
Haifa 32000, Israel

Introduction

IN order to account for unsteady aerodynamics in first-order, time-invariant state-space formulation of aeroelastic equations of motion, the aerodynamic forces have to be described as a rational function in the Laplace domain. The

Minimum-State (MS) aerodynamic approximation method^{1,2} was designed to minimize the number of aerodynamic states in the resulting aeroelastic model. References 2 and 3 applied the MS method to subsonic aeroservoelastic problems with one flutter mechanism and demonstrated a reduction of about 75% of the number of aerodynamic states relative to other methods with the same level of accuracy. The effectiveness of the MS method was increased by the introduction of a physical weighting technique² which weights each aerodynamic input data term according to its relative importance. Reference 4 used the MS formulation for additional reduction of the model size by dynamic residualization of high frequency structural states. The MS and the physical weighting procedures are extended in this Note to expand their efficiency and generality and to improve the dynamic residualization. Even though the formulation and numerical examples deal with structural-mode-related aerodynamics only, the extensions are applicable to control surface and gust related aerodynamics as well.

Minimum-State Approximation Procedure

The MS method approximates the Laplace domain generalized aerodynamic force coefficient matrix by:

$$[\tilde{Q}_s(p)] = [A_0] + [A_1]p + [A_2]p^2 + [D](p[I] - [R])^{-1}[E]p \quad (1)$$

where p is the nondimensionalized Laplace variable $p = sb/V$, where b is a reference length and V is the true airspeed. The resulting time-domain state-space aeroelastic equations of motion are presented in Ref. 2. The number of aerodynamic states m is equal to the order of $[R]$.

The input data are unsteady aerodynamic complex matrices $[Q_s(ik_i)] = [F(k_i)] + i[G(k_i)]$, calculated at several $p = ik_i$ points where each $k_i = \omega_i b/V$ is a tabulated reduced frequency. The approximation problem is to find the combination of the real valued $[A_0]$, $[A_1]$, $[A_2]$, $[R]$, $[D]$, and $[E]$ of Eq. (1) that best fit the tabulated data. The $m \times m$ aerodynamic lag matrix $[R]$ is diagonal with distinct negative values to be chosen by the analyst. The applications of Refs. 2 and 4 indicated that the results are not very sensitive to the lag values when they are spread over the range of tabulated k_i values. Three approximation constraints are applied to each term of $[Q_s]$ in order to reduce the problem size by explicitly determining $[A_0]$, $[A_1]$, and $[A_2]$. The formulation of Ref. 2 is extended here to allow more flexibility in constraint selection without increasing the problem size. The three constraints are: 1) data match at $k_i = 0$, which yields

$$A_{0ij} = F_{ij}(0) \quad (2)$$

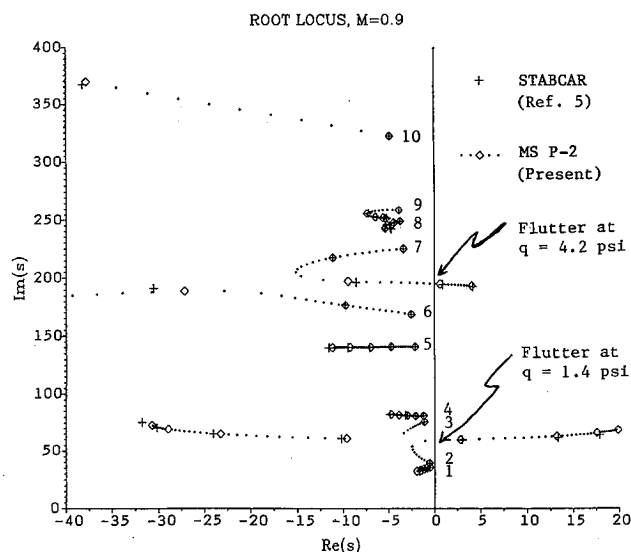


Fig. 1 Comparison of root loci generated by minimum-state and the p - k methods, flexible wing at $M = 0.9$.

Received March 12, 1990; revision received Aug. 2, 1990; accepted for publication Aug. 25, 1990. Copyright © 1990 by the American Institute of Aeronautics and Astronautics, Inc. All rights reserved.

*Associate Professor, Faculty of Aerospace Engineering. Member AIAA.

Table 1 Maximal weighted magnitudes of the aerodynamic data terms

$i =$	1	2	3	4	5	6	7	8	9	10
$j = 1$	0.098	0.126	0.086	0.012	0.000	0.018	0.007	0.001	0.006	0.005
2	0.137	<u>1.000</u>	0.707	0.038	0.007	0.129	0.104	0.008	0.079	0.045
3	0.085	0.722	<u>0.622</u>	0.052	0.003	0.091	0.039	0.003	0.029	0.015
4	0.010	0.059	0.044	0.022	0.001	0.006	0.003	0.000	0.002	0.000
5	0.001	0.003	0.004	0.002	0.043	0.002	0.001	0.000	0.001	0.001
6	0.027	0.132	0.115	0.013	0.002	<u>0.377</u>	0.026	0.003	0.012	0.060
7	0.013	0.079	0.053	0.006	0.001	0.042	<u>0.274</u>	0.004	0.028	0.066
8	0.001	0.008	0.005	0.000	0.000	0.003	0.003	0.018	0.002	0.001
9	0.011	0.070	0.041	0.006	0.001	0.023	0.031	0.003	0.135	0.090
10	0.007	0.046	0.021	0.007	0.001	0.087	0.087	0.000	0.098	<u>0.291</u>

2) real-part data-match at a nonzero $k_l = k_f$, or a zero coefficient constraint, which yields

$$A_{2ij} = [F_{ij}(0) - F_{ij}(k_f)]/k_f^2 + \{D_i\}^T \{k_f^2 [I] + [R]^2\}^{-1} \{E_j\} \quad (3a)$$

or

$$A_{2ij} = 0 \quad (3b)$$

where $\{D_i\}^T$ is the i th row of $[D]$ and $\{E_j\}$ is the j th column of $[E]$; and 3) imaginary-part data-match at a nonzero $k_l = k_g$, or a zero coefficient constraint, which yields

$$A_{1ij} = G_{ij}(k_g)/k_g + \{D_i\}^T \{k_g^2 [I] + [R]^2\}^{-1} [R] \{E_j\} \quad (4a)$$

or

$$A_{1ij} = 0 \quad (4b)$$

The approximation formula (1) and the constraint equations (2–4) yield an over-determined set of approximate equations which are solved for $[D]$ and $[E]$ by an iterative, weighted, least-square procedure, which starts with an initial guess of $[D]$. The equations and the solution procedure are those of Ref. 2, modified to allow k_f of Eqs. (3) and k_g of Eqs. (4) to have different values for different aerodynamic terms, and to allow the data-match constraints to be replaced by zero coefficient constraints.

Approximation Constraints for Subsequent Dynamic Residualization

The MS aeroelastic model is used in Ref. 4 for a further reduction of the model size via dynamic residualization, which eliminates the states associated with a subset of high-frequency vibration modes, but retains most of their effects on the retained states. The coefficient matrices of Eq. (1) are partitioned into the retained r and eliminated e partitions:

$$[A_i] = \begin{bmatrix} A_{irr} & A_{ire} \\ A_{ier} & A_{iee} \end{bmatrix} \quad \text{for } i = 0, 1, 2; \quad [D] = \begin{bmatrix} D_r \\ D_e \end{bmatrix} \quad (5)$$

$$[E] = [E_r \quad E_e]$$

Unlike the static residualization, which neglects all of the e -related partitions except for the A_0 terms, the dynamic residualization neglects only the A_{1ee} , A_{2ee} , A_{2er} , and A_{2re} terms. The retained effects of A_{1er} , A_{1re} , D_e , and E_e improve the accuracy of the residualized model without increasing its size. The attempt made in Ref. 4 to improve the dynamic residualization even further by constraining the neglected terms to be zero in the preceding MS procedure (in lieu of data-match constraints) did not yield better results. The reason was that with $A_{1ee} = 0$ the approximation errors are increased significantly. This had a negative effect on the quality of the entire approx-

imated aerodynamics (including that of the retained modes) because the MS procedure minimized a single total error parameter. The modification suggested here is to apply the least-square solutions for $[E_r]$ and $[D_r]$ with the data associated with the retained modes only. The $[D_e]$ and $[E_e]$ matrices are solved with the entire data. As a result, the approximated $[\tilde{Q}_{s,r}]$ is not affected by the inclusion of the eliminated modes in the approximation procedure.

Physical Weighting

A physical weighting method that weights each term of the tabulated aerodynamic data according to a "measure of importance" is presented in Ref. 2. The measure-of-importance matrix associated with $[Q_s(ik_l)]$ is

$$[\tilde{W}]_l = \left| \left(-[M_s]k_l^2 + i[B_s]k_l + [K_s] + q_n[Q_s(ik_l)] \right)^{-1} \right|^T \quad (6)$$

where $[M_s]$, $[B_s]$, and $[K_s]$ are the generalized mass, damping and stiffness matrices and q_n is a nominal dynamic pressure. As shown in Refs. 2 and 3, the variations of the measure-of-importance terms of Eq. (6) with k may have very sharp peaks. In addition, the peak values of many terms may be several orders-of-magnitude smaller than other peaks. The resulting extreme variations of weights may cause unrealistic approximation curves. To ensure good results at k values that fall between the tabulated ones, and to facilitate the application of the resulting aeroelastic model to a variety of flow conditions, structural modifications, and control parameters, it may be desired to widen the weight peaks and to scale up the extremely low weights. The peak widening is performed in n_{wd} cycles where, in each cycle, $\tilde{W}_{ij}(k_l)$ is changed to be $\max\{\tilde{W}_{ij}(k_{l-1}), \tilde{W}_{ij}(k_l), \tilde{W}_{ij}(k_{l+1})\}$ of the previous cycle. The weights to be applied in the MS procedure are then calculated by

$$W_{ijl} = \tilde{W}_{ijl} \left(\max \left\{ \frac{1}{\max_{i,j} \{\tilde{W}_{ij}\}}, \frac{W_{cut}}{\tilde{W}_{ij}} \right\} \right) \quad (7)$$

where

$$\tilde{W}_{ij} = \max_l \left\{ \left| Q_{s,ij}(ik_l) \right| \tilde{W}_{ijl} \right\}$$

and where W_{cut} is defined by the analyst. In this way, the maximum weighted absolute value of each aerodynamic term falls between W_{cut} and 1.

Numerical Examples

The numerical examples deal with the mathematical model of the active flexible wing (AFW) wind-tunnel model (described in Ref. 4) with symmetric boundary conditions at Mach 0.9. The doublet lattice tabulated oscillatory aerodynamic matrices were generated at 12 k_l values between 0.0 and 2.0 using the STABCAR⁵ computer code, which was also

employed to calculate the baseline p -plane roots using the p - k method with 10 vibration modes. The resulting root-locus plots are shown in Fig. 1, which indicates two flutter mechanisms. The flutter dynamic pressure and frequency of the first mechanism (second branch) are $q_f = 1.447$ psi and $\omega_f = 58.94$ rad/s ($k_{flut} = 0.21$). The flutter results of the second mechanism (seventh branch) are $q_f = 4.247$ psi and $\omega_f = 194.43$ rad/s ($k_{flut} = 0.69$).

The physical weightings were performed with $q_n = 1.2$ psi. Two types of physical weightings are compared below. The first type (symbolized by $P-0$) is with the original measures-of-importance of Eq. (6), namely with no peak widening ($n_{wd} = 0$) and with no upscaling [$W_{cut} = 0$ in Eq. (7)]. The second type (symbolized by $P-2$) is with the two peak-widening cycles ($n_{wd} = 2$) and with $W_{cut} = 0.01$. The maximal weighted magnitudes of the $P-0$ aerodynamic data terms are given in Table 1. The most important modes are 2, 3, 6, 7, and 10, which have the highest diagonal values. The off-diagonal values associated with these modes are also higher than those of most other terms. It can be noticed that about 50% of the terms in Table 1 are smaller than 0.01. These terms are scaled up to 0.01 in the $P-2$ case. Comparison of Table 1 with the aeroelastic behavior of Fig. 1 indicates that the weighting is reasonable over the entire q range of interest.

The flutter characteristics of the resulting state-space models have been found by a linear root-locus analysis with variable q . The quality of the approximations is evaluated by comparing the state-space results with the STABCAR results. An overall measure in each case is the rms value of the percentage errors in the four flutter parameters (q_f , ω_f , q_{f2} , and ω_{f2}). Comparisons between rms flutter errors in nonweighted cases (N) and physically weighted ($P-0$ and $P-2$) cases are shown in Fig. 2. It can be observed that the $P-2$ cases generally yield the best results and that they are more consistent than the $P-0$ cases. Calculations at Mach 1.15 (not shown) exhibit similar results.

The root locus of the $P-2$ case with six aerodynamic lags, $\text{diag}[R] = \{-0.2, -0.45, -0.8, -1.2, -1.7, -2.0\}$ is compared in Fig. 1 to that of the reference STABCAR solution. It can be observed that the agreement is good over the entire ranges of frequency, damping, and dynamic pressure. This indicates that the physical weights calculated at q_n are adequate over the entire range.

All of the preceding MS cases were constrained to match the data at $k = 0.0$ and at the highest tabulated reduced frequency, namely $k_f = k_g = 2.0$. Data-match constraints at k_f values close to either one of the two k_{flut} values caused a slight improvement in the respective flutter mechanism, but a slight increase of the overall rms error measure by about 1%. An error increase of about 2% was obtained when $[A_2] = [0]$ replaced

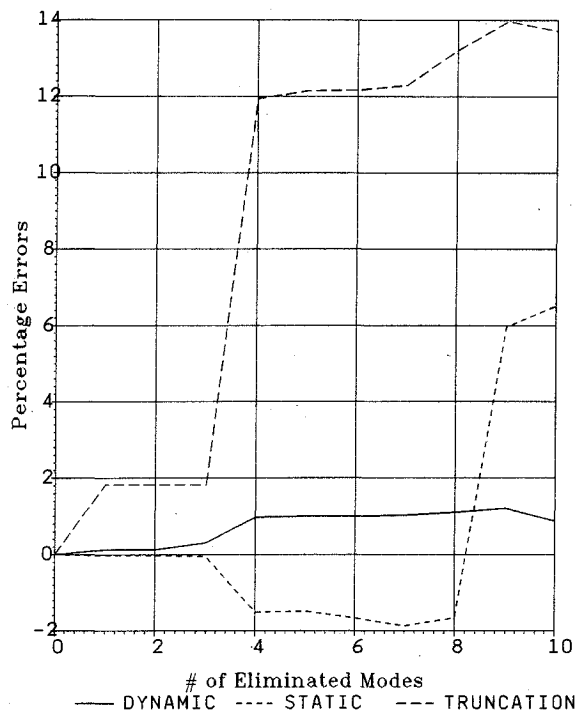


Fig. 3 Effect of various methods of modal reduction on the error in the predicted flutter dynamic pressure of the second flutter mechanism.

the k_f constraints. Much more significant errors resulted from the replacement of the k_g constraints by $A_1 = 0$ even when applied to the aerodynamic terms associated with the highest frequency mode only. These errors were reduced considerably with the application of the new procedure for subsequent dynamic residualization.

To demonstrate the application of the modified MS approximations in subsequent flutter analysis with dynamic residualization, the $P-2$ model with six aerodynamic states has been extended to include the first 20 vibration modes (instead of 10). The MS approximations were performed with the special residualization constraints assigned to the last 10 modes. The reference case is flutter analysis with all the 20 vibration modes. Reduced-size flutter analyses were performed by eliminating a subset of high-frequency modes by either mode truncation, static residualization, or dynamic residualization. Variations of flutter dynamic pressure percentage errors vs number of eliminated modes are shown in Fig. 3 for the second flutter mechanism. Similar trends, but with smaller errors, were obtained for the first flutter mechanism. These results demonstrate that MS aerodynamic approximations facilitate additional high-accuracy model size reduction via dynamic residualization.

References

- ¹Karpel, M., "Design for Active Flutter Suppression and Gust Alleviation Using State-Space Aeroelastic Modeling," *Journal of Aircraft*, Vol. 19, No. 3, 1982, pp. 221-227.
- ²Karpel, M., "Time-Domain Acroservoelastic Modeling Using Weighted Unsteady Aerodynamic Forces," *Journal of Guidance, Control, and Dynamics*, Vol. 13, No. 1, 1990, pp. 30-37.
- ³Tiffany, S. H., and Karpel, M., "Aeroservoelastic Modeling and Applications Using Minimum-State Approximations of the Unsteady Aerodynamics," *Proceedings of the AIAA/ASME/ASCE/AHS/ASC 30th Structures, Structural Dynamics, and Materials Conference*, AIAA, Washington, DC, 1989, pp. 265-274.
- ⁴Karpel, M., "Reduced-Order Aeroelastic Models via Dynamic Residualization," *Journal of Aircraft*, Vol. 27, No. 5, 1990, pp. 449-455.
- ⁵Adams, W. M., Jr., Tiffany, S. H., Newsom, J. R., and Peele, E. L., "STABCAR—A Program for Finding Characteristic Roots of Systems Having Transcendental Stability Matrices," NASA TP 2165, June 1984.

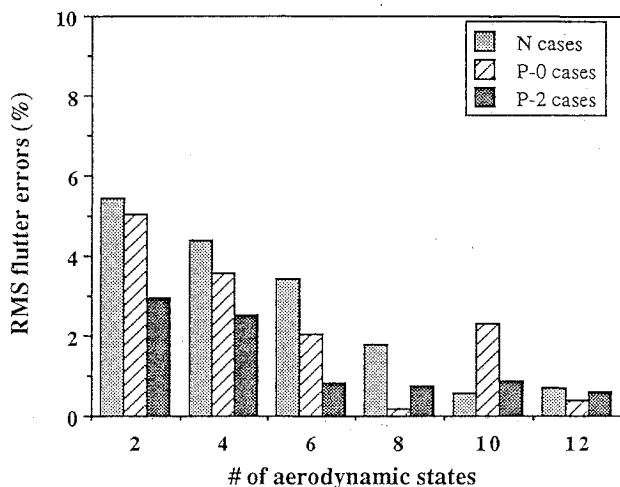


Fig. 2 RMS flutter errors resulting from minimum-state aerodynamic approximations.